

Fragile X premutation RNA is sufficient to cause primary ovarian insufficiency in mice

Cuiling Lu¹, Li Lin², Huiping Tan², Hao Wu³, Stephanie L. Sherman², Fei Gao¹, Peng Jin^{2,*} and Dahua Chen^{1,*}

¹State Key Laboratory of Reproductive Biology, Institute of Zoology, Chinese Academy of Sciences, Beijing, P.R. China, ²Department of Human Genetics, Emory University School of Medicine and ³Department of Biostatistics and Bioinformatics, Emory University Rollins School of Public Health, Atlanta, GA 30322, USA

Received May 22, 2012; Revised and Accepted August 15, 2012

Spontaneous 46,XX primary ovarian insufficiency (POI), also known as ‘premature menopause’ or ‘premature ovarian failure’, refers to ovarian dysfunction that results in a range of abnormalities, from infertility to early menopause as the end stage. The most common known genetic cause of POI is the expansion of a CGG repeat to 55–199 copies (premutation) in the 5′ untranslated region in the X-linked fragile X mental retardation 1 (*FMR1*) gene. POI associated with the *FMR1* premutation is referred to as fragile X-associated POI (FXPOI). Here, we characterize a mouse model carrying the human *FMR1* premutation allele and show that *FMR1* premutation RNA can cause a reduction in the number of growing follicles in ovaries and is sufficient to impair female fertility. Alterations in selective serum hormone levels, including FSH, LH and 17β-estradiol, are seen in this mouse model, which mimics findings in humans. In addition, we also find that LH-induced ovulation-related gene expression is specifically altered. Finally, we show that the *FMR1* premutation allele can lead to reduced phosphorylation of Akt and mTOR proteins. These results together suggest that *FMR1* premutation RNA could cause the POI associated with *FMR1* premutation carriers, and the Akt/mTOR pathway may serve as a therapeutic target for FXPOI.

INTRODUCTION

Spontaneous 46,XX primary ovarian insufficiency (POI), also known as ‘premature menopause’ or ‘premature ovarian failure’ (POF), refers to ovarian dysfunction that results in a range of abnormalities, from infertility to early menopause as the end stage (1). Independent of its etiology, POI manifests as ovarian dysfunction along a continuum of severity. The most severe form of this condition, POF, affects ~1% of women by age 40 and 0.1% of women by age 30 (1). The reduced ovarian function characteristic of POI causes estrogen deficiency that may result in clinical symptoms, such as hot flashes, vaginal dryness and insomnia, as well as negative effects on cardiovascular health and decreased bone mineral density (2–5). Currently, the only mouse model to study POI and menopause is the VCD-induced model, in which the industrial chemical 4-vinylcyclohexene diepoxide is used to induce the menopause state (6).

Fragile X syndrome (FXS), the most common form of intellectual and developmental disabilities, is caused by expansion of CGG trinucleotide repeat in the 5′ untranslated region of the fragile X mental retardation 1 (*FMR1*) gene, which leads to silencing of its transcript and loss of the encoded fragile X mental retardation protein (FMRP) (7–12). Most affected individuals have more than 200 rCGG repeats, referred to as full mutation alleles (13). Individuals with 55–199 repeats (termed ‘premutation’) typically do not show symptoms of FXS, but are at risk of a late-onset tremor/ataxia disorder (FXTAS) and, for women, are at risk for fragile X-associated POI (FXPOI) (14). POI begins with unusually early hormonal changes, such as elevated levels of FSH, despite normal menstrual cycles, and culminates in menopause before the age of 40. POI occurs in <1% of the general female population, but up to 24% of *FMR1* premutation carriers are affected (15,16). As a group, women who carry the *FMR1* premutation alleles experience menopause ~5 years earlier than non-carriers

*To whom correspondence should be addressed. Email: chendh@ioz.ac.cn (D.C.) or peng.jin@emory.edu (P.J.)

(17,18). The effects of the premutation reach beyond reproductive implications, however, to affect all female carriers, because in addition to the early loss of fertility, these women face the potential early onset of serious conditions associated with early estrogen deficiency, including a heightened risk of osteoporosis and cardiovascular disease. Indeed, FXPOI is the most common known genetic causes of 46,XX POI, and the *FMRI* premutation accounts for 4–6% of all cases of 46,XX POI (14). Genetic epidemiology studies suggest that the onset and severity of ovarian dysfunction associated with FXPOI is variable, and could potentially be modulated by the CGG repeat length and additional genetic and environmental factors (14).

There are several known molecular consequences of the *FMRI* premutation alleles. They are genetically unstable and can expand to the full mutation during germline transmission (19). Large premutation alleles lead to the reduced production of FMRP due to the long CGG repeat track in the RNA (rCGG) that is thought to impede translation initiation complex (20). One unique molecular signature of the *FMRI* premutation allele is that the level of *FMRI* mRNA is significantly elevated (8,21). Multiple lines of evidence point to the neurodegenerative phenotypes associated with FXTAS being caused by a gain of function in *FMRI* premutation rCGG repeat RNAs (19,22–25). The hypothesis is that overproduced rCGG repeats in FXTAS sequester specific RNA-binding proteins and reduce their ability to perform their normal cellular functions, thereby contributing significantly to the pathology of this disorder. Two RNA-binding proteins, Pur α and hnRNP A2/B1, were found to bind rCGG repeats specifically in both mammalian and *Drosophila* brains (26,27). However, the molecular mechanisms underlying how the *FMRI* premutation alleles disrupt ovarian function and cause the phenotype of early menopause are still a mystery. Whether *FMRI* rCGG repeats, altered expression of FMRP, or both contribute to FXPOI remains to be determined.

Here, we characterize a mouse model carrying the human *FMRI* premutation allele and show that *FMRI* premutation RNA is sufficient to impair female fertility. We find that *FMRI* premutation RNA can cause a reduction in the number of growing follicles in ovaries, but not affect primordial follicles. Alterations in selective serum hormone levels, including FSH, LH and 17 β -estradiol (E₂), are seen in this mouse model, which mimics the findings in humans. In addition, we also find that LH-induced ovulation-related gene expression is specifically altered. Finally, we show that the *FMRI* premutation allele can lead to reduced phosphorylation of Akt and mTOR proteins. These results together suggest that *FMRI* premutation RNA could cause POI among premutation carriers, and the Akt/mTOR pathway may serve as a therapeutic target for FXPOI. Our mouse model represents the first genetic model of human early menopause.

RESULTS

Fragile X premutation RNA impairs female fertility

To explore the potential role of the *Fmr1* gene in controlling female fertility, we examined *Fmr1* RNA expression by *in situ* hybridization and Fmrp expression by immunohistochemistry

at different developmental stages. We saw that both the *Fmr1* mRNA and protein were presented predominantly in granulosa cells (GCs) and oocytes of all types of follicles (from primordial follicles to mature follicles) versus that in ovarian interstitial cells in adult mice ovary (Fig. 1A). To further study the molecular basis of FXPOI, we used a previously developed transgenic mouse line that carries the premutation CGG repeat allele (28). In this mouse model, a human yeast artificial chromosome (YAC) carrying the *FMRI* locus with a premutation of 90 CGG repeats inserted through homologous recombination was used to generate the transgenic mouse (TG296). We examined the mRNA and protein levels of the *FMRI* gene in the ovary of this fragile X premutation transgenic line. Surprisingly, we saw a significantly increased mRNA level, but not protein level, in the ovary (Supplementary Material, Fig. S1).

To investigate whether the *FMRI* premutation allele could affect female fertility, we crossed age-matched wild-type (WT) and TG296 (premutation) females with WT males that have normal fertility. Females were housed with males starting at 8 weeks of age and monitored continuously for 10 months. Among 11 randomly selected premutation females, 3 were sterile and never yielded litters, whereas the others gave birth to a smaller cumulative number of pups, compared with the WT controls (37.1 versus 77; Fig. 1B). We noted that the sub-fertility of premutation females was apparently attributable to two different factors. First, the premutation females delivered their first litter \sim 1 month later than WT females did (12.5 ± 2.7 versus 8.5 ± 0.7 weeks of age; Fig. 1C). Second, the average number of pups per litter was significantly reduced in the premutation females versus WT controls (4.9 ± 2.5 versus 12.4 ± 3.68 ; Fig. 1D). We further examined the body weight and uterine weight of the premutation and WT animals. We found that, while the WT females showed a significant increase in body weight from 9 to 22 weeks of age (from 24.2 ± 2 to 36.3 ± 0.3 g) (mean \pm SD), the premutation females had only a small increase (from 21.15 ± 2.8 to 30.6 ± 1.5 g) (mean \pm SD) during the same testing period (Fig. 1E). The measurement of the uterine weight of both types of mice showed that the ratio between uterine and body weight of premutation females was significantly lower than that for WT controls ($P < 0.05$) at 9 weeks (Fig. 1F). These findings suggest that the reduced uterine weight might be a specific phenotype in premutation females, but not a reflection of their decreased body size, pointing to a specific defect caused by the premutation in the reproductive system. Given that the *Fmrp* level is not significantly altered in premutation mice versus WT mice, our data also suggest that fragile X premutation RNA could impair female fertility.

Reduced number of growing follicles in fragile X premutation ovaries

To determine whether the *FMRI* premutation allele could influence ovarian development and alter ovarian function, we analyzed the morphology of the ovaries of fragile X premutation females at different ages using WT littermate females as controls. At postnatal days 8 (PD8) and 25 (PD25), the dimensions of the premutation ovaries are similar to those of WT (Fig. 2A). The ovaries of premutation females at PD25

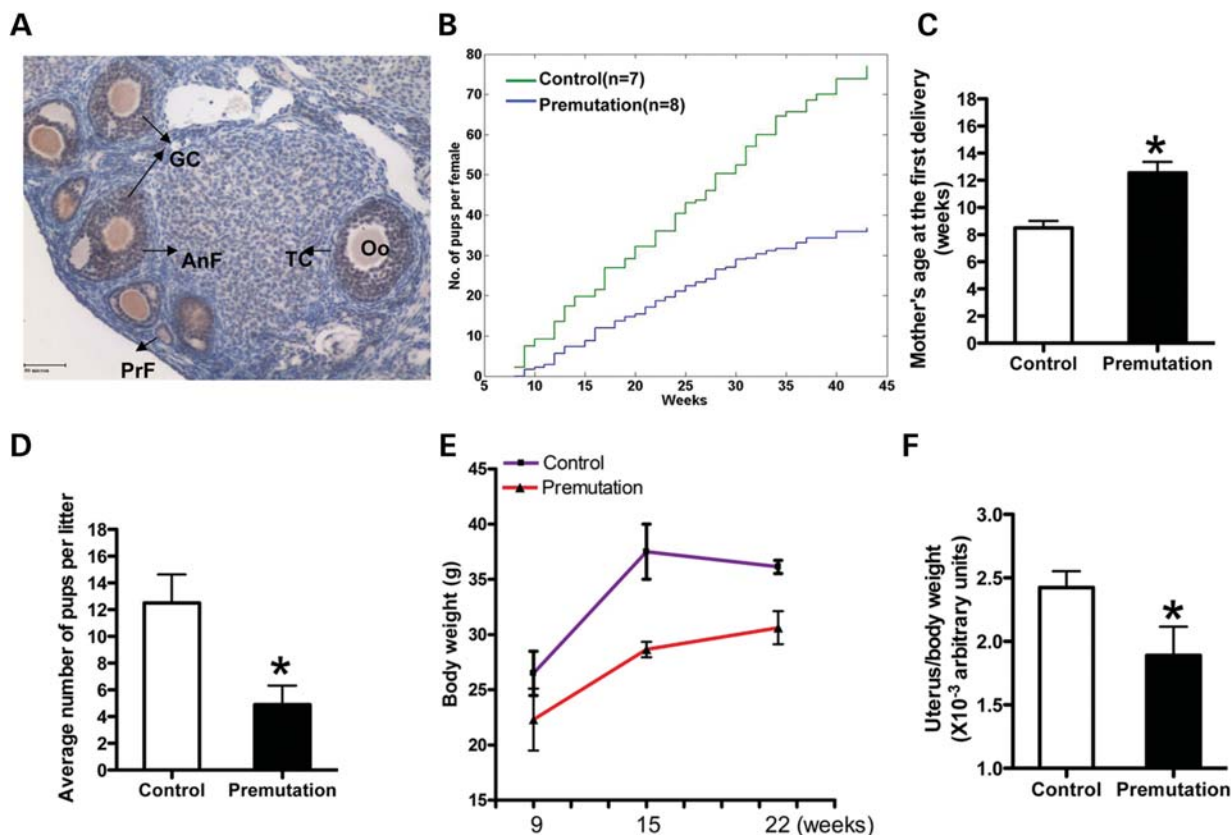


Figure 1. Fragile X premutation RNA impairs female fertility. (A) immunohistochemistry staining of *Fmrp* in the ovary of a 9-week-old WT mouse. Brown staining indicates immunoreactivity and nuclei are counterstained blue. Bar: 50 μm . GC, granulosa cell; Oo, oocyte; TC, theca cell; AnF, antral follicle; PrF, primary follicle. (B) Lifespan breeding assays started at \sim 8 weeks of age. Comparison of the cumulative number of pups per fragile X premutation (TG296-Premutation) female (blue line) and per WT littermate (green line), $n = 7$ for WT mice, $n = 8$ for TG296 mice. (C) the ages of mothers at first delivery (mean \pm SD). (D) the litter sizes of WT and premutation females (mean \pm SD). $N = 13$ for premutation mice, $n = 9$ for WT mice. (E) the body weights of females at different ages (mean \pm SD). (F) Graph of the uterus/body weight ratio of females at 9 weeks of age (mean \pm SD). Statistical significance ($*P < 0.05$) was calculated by Student's *t*-test.

showed a comparable number of immature follicles as the WT ovaries. We then quantified the number of cells from the different stages of oocyte and follicle development on the basis of the widely used classification developed by Pedersen and Peters (29) previously at PD25 and at 9 weeks. In this classification, follicle cells were divided into eight subgroups on the basis of: (i) the size of the oocytes in follicles at different stages of development, (ii) the size of the follicles defined by the number of cells constituting the follicular envelope and (iii) the morphology of the follicles. Compared with WT ovaries, we found that the number of type 6 follicles (the mature follicles) was significantly reduced in PD25 premutation females ($P < 0.05$; Fig. 2B). The reduction of type 6 follicles was also seen in 9-week-old premutation females as well ($P < 0.05$; Fig. 2C), indicating that proper follicle development could not recover in adult premutation ovaries. Notably, the number of type 7 follicles and corpus luteum (CL) were also significantly reduced in 9-week-old premutation females ($P < 0.001$; Fig. 2C). In addition, the numbers of types 3, 4 and 5 follicles in adult premutation females were also less than in WT littermates, although this was not statistically significant ($P > 0.05$). Consistent with these observations, further morphological analysis revealed that

the *FMRI* premutation females had smaller ovaries at 9 and 16 weeks versus their WT littermates (Fig. 2A). Interestingly, we found that primordial follicles, the type 1 and 2 follicles, which represent the oocyte reservoir, were not apparently affected by the fragile X premutation allele. Taken together, these results suggest the fragile X premutation allele could alter ovarian function, probably by impairing the development of the growing follicles, but not affecting primordial follicles.

Altered serum hormone levels in fragile X premutation mice

Since impaired ovarian function was usually linked to abnormal levels of sex steroid and non-steroid hormones, such as FSH and LH, we sought to examine the serum hormone levels of FSH, LH and $17\beta\text{-E}_2$ in *FMRI* premutation mice (14). Using the protocol that was developed and published previously, we sacrificed the adult WT and *FMRI* premutation littermate female mice from 9 to 22 weeks at the proestrus stage (based on vaginal smears), and serum hormone FSH, LH and $17\beta\text{-E}_2$ levels were determined by radioimmunoassay. As shown in Fig. 3A, the premutation mice exhibited apparently higher levels of E_2 than WT littermates at 10–12 weeks of

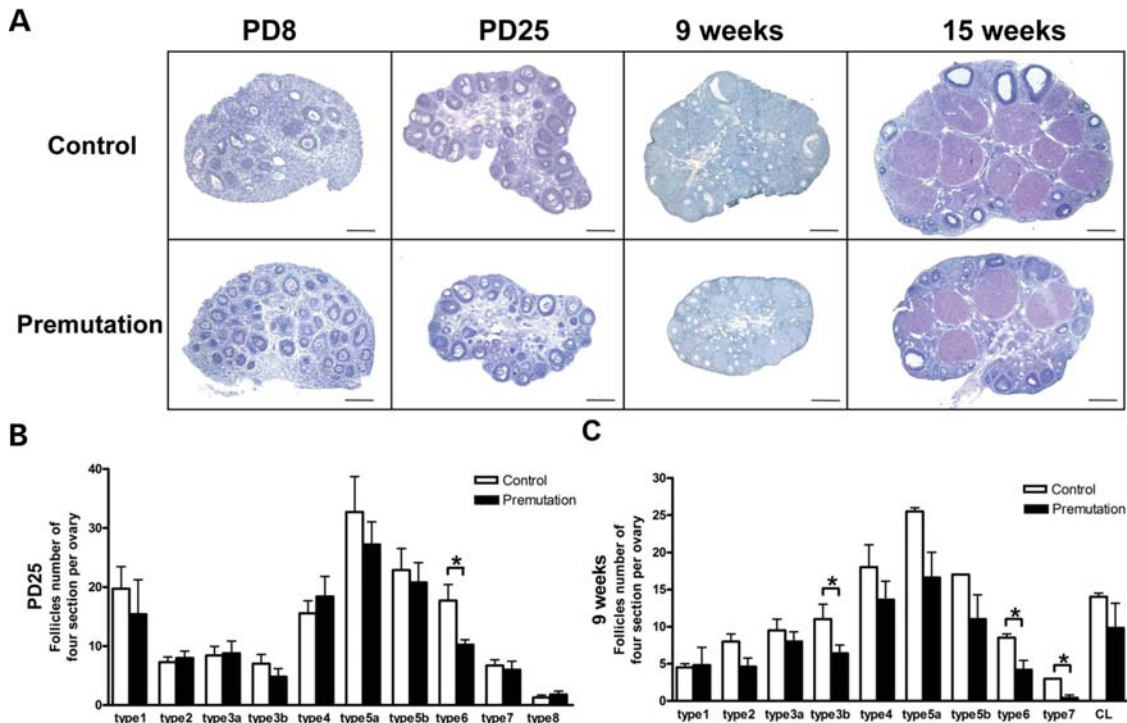


Figure 2. Reduced number of growing follicles in fragile X premutation ovaries. (A) Histology of ovarian sections from premutation and WT littermates of PD8, PD25, 9- and 15-week-old females stained with hematoxylin/eosin dye (bar: 200 μ m). (B and C) the quantifications of numbers for each type of follicle cell at PD25 and 9 weeks. The experiments were repeated four times, and for each time and each age, ovaries from three mice of each genotype were used. Relative follicle counts at PD25 (B) and 9 weeks (C) of age for premutation mice and WT littermates. Numbers represent the four serial biggest sections from every fifth section per sectioned ovaries ($n = 5$ animals per genotype). For all panels, data are shown as mean \pm SEM, and statistical significance ($*P < 0.05$) was calculated by Student's *t*-test.

age; however, the premutation mice showed levels of E_2 similar to those found in WT littermates between 16 and 22 weeks of age. This was consistent with artificial ovulation induced by exogenous hormones [pregnant Mare's serum gonadotropin (PMSG) and human chorionic gonadotropin (hCG)]. There were no differences in the numbers and sizes of the ovulated oocytes between WT and premutation mice, suggesting that the ovaries from both mice could respond to the hormone stimulation similarly (Supplementary Material, Fig. S2). Continuously from 9 to 22 weeks, the levels of serum FSH were significantly higher in the premutation mice than in WT littermates (Fig. 3B). The serum LH level in adult premutation females was significantly lower than in the WT littermates (Fig. 3C). Taken together, our data suggest that *FMRI* premutation mice display abnormal levels of serum hormones, reminiscent of what has been observed in FXPOI patients. It is possible that the activation of the pool of primordial follicles by FSH leads to follicle depletion, and the lower level of LH causes decreased ovulation in *FMRI* premutation ovaries.

Increased apoptosis of follicle cells in fragile X premutation ovaries

Given that the serum FSH level is abnormally high in premutation mice and that the number of follicles is decreased, we reasoned that the decrease in follicles in premutations could be due to increased atresia. We therefore performed terminal

deoxynucleotidyl transferase-mediated biotinylated UTP nick end labeling (TUNEL) assays to analyze ovarian sections from mice of different ages (PD35, 16 weeks, 22 weeks). As shown in Fig. 2A, WT ovaries showed an abundance of healthy follicles with tightly attached and well-organized granulosa cell and theca cell layers, which exhibited negative TUNEL staining (Fig. 4). By contrast, many of the antral follicles in *FMRI* premutation ovaries appeared atretic as characterized by the presence of detached granulosa cell layers and strong positive TUNEL staining (Fig. 4), suggesting that the *FMRI* premutation allele could induce increased apoptosis in ovaries.

Altered expression of the LH-induced ovulation-related genes in fragile X premutation ovaries

To analyze the altered gene expression in *FMRI* premutation ovaries, we collected ovaries from PD25 and proestrus-stage adults (from 8 to 14 weeks old) of both WT and *FMRI* premutation mice. Consistent with our findings in serum hormone levels, LH receptor (*Lhr*) was significantly downregulated in both PD25 mice and proestrus-stage adults. Surprisingly, there were no significant alterations in the mRNA level in *FMRI* premutation ovaries at either stage associated with FSH receptor (*Fshr*), 17- α -hydroxylase (*Cyp17a1*), aromatase (*Cyp19*), estrogen receptor- β (*Esr2*), Cyclin D2 (*Ccnd2*) or insulin-like growth factor 1 (*Igf1*), which are the other major known regulators and markers of folliculogenesis

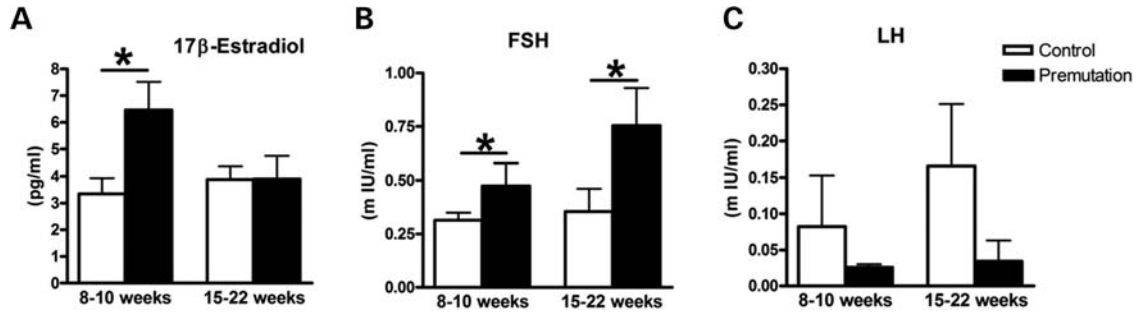


Figure 3. Altered serum hormone levels in fragile X premutation mice. The elevated levels of estradiol (A) and FSH (B) and the decreased level of LH (C) in adult premutation versus WT littermates. On average, 8–11 mice were used for each time point and each genotype. Female mice of both genotypes were sacrificed at the proestrus stage, and sera were collected for measurement of 17β-estradiol, FSH and LH levels. Statistical significance ($*P < 0.05$) was calculated by Student's *t*-test.

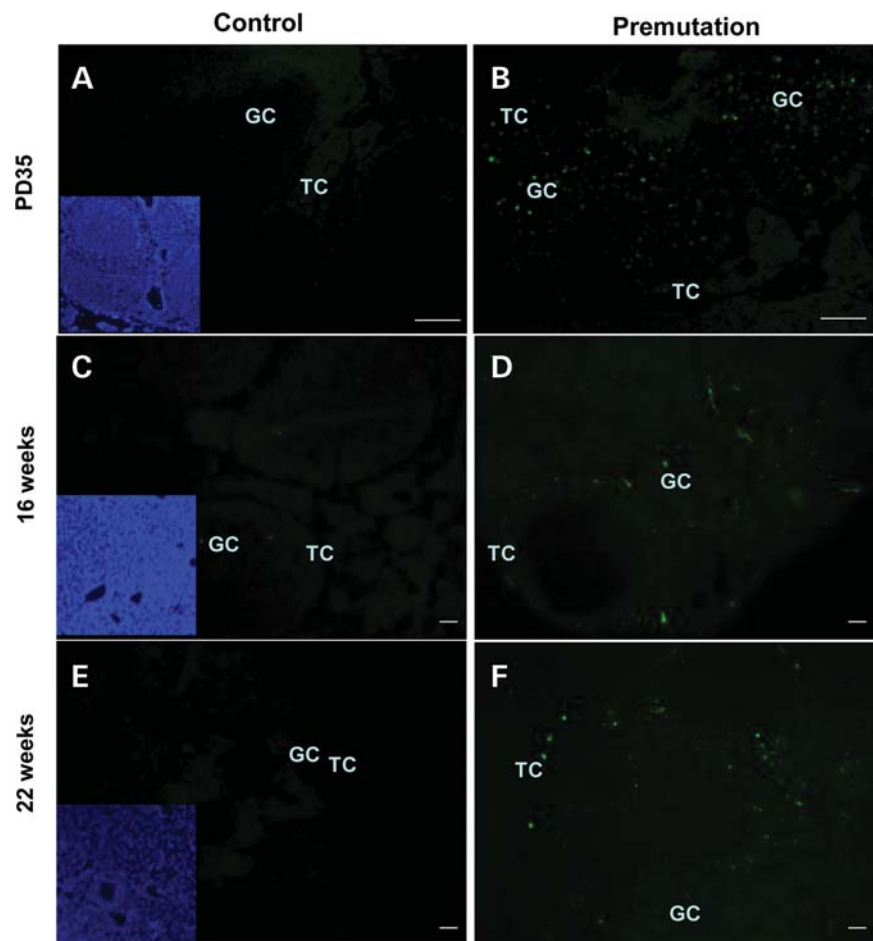


Figure 4. Increased apoptosis of follicle cells in fragile X premutation ovaries. Follicular apoptosis was detected by TUNEL on serial sections. Atresic follicles and cells exhibited positive TUNEL staining, whereas healthy ones were TUNEL negative. Representatives of slides from six animals are shown. Bar: 50 μ m. TC, theca cell; GC, granulosa cell; inset denotes nuclear staining by Hoechst.

besides *Lhr* (Fig. 5A and B). In addition, we saw a large number of LH-induced ovulation-related genes downregulated specifically at the proestrus stage in adults, including *Areg*, *Edn2*, *Ereg*, *Has2*, *IL6* and *Ptgs2* (Fig. 5B). These analyses suggest that the LH-mediated biological pathway could be affected in *FMR1* premutation ovaries.

Reduced phosphorylation of Akt and mTOR in fragile X premutation ovaries

It is well known that the PI3K-Akt pathway can regulate many aspects of cell function, including cell-cycle progression/arrest, DNA repair and apoptosis (30). The critical roles of the PI3K pathway in gonadotropin-mediated GC differentiation,

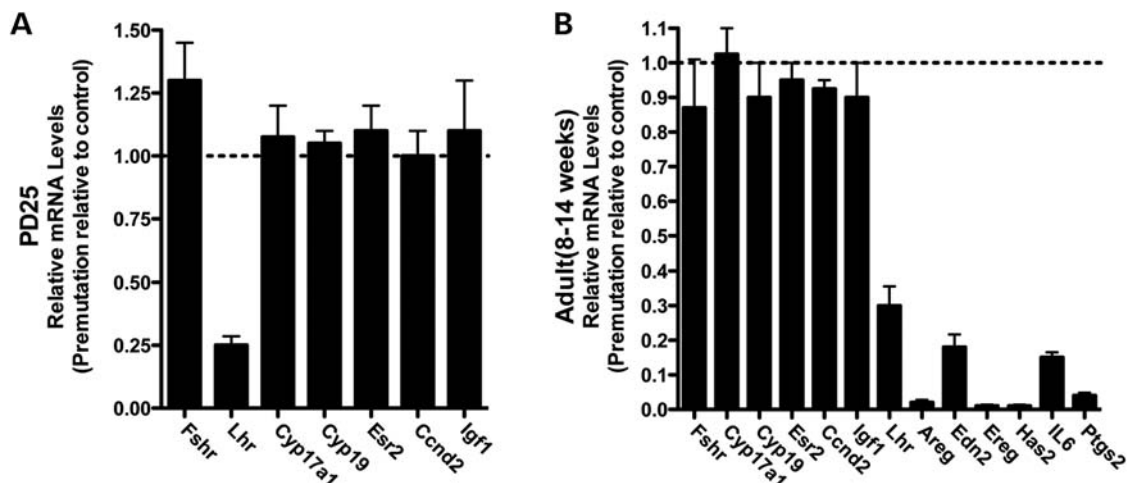


Figure 5. Altered expression of the LH-induced ovulation-related genes in fragile X premutation ovaries. The ovaries from both premutation and WT littermates at PD25 and 10–14 weeks of age were collected for gene expression analyses. Results shown are the representative real-time PCR results (using two or three ovaries per genotype in each experiment) of three independent experiments. Data were analyzed by using Student's *t* test and are shown as mean \pm SEM.

cumulus expansion and oocyte maturation have been demonstrated previously (31–33). Akt is known to play an instrumental role in the regulation of growth and maturation of the ovary, and the loss of Akt can lead to POF (34). Given the ovarian phenotypes associated with fragile X premutation mice, we examined the level of both phosphorylated and overall Akt proteins. We saw a significant reduction of phosphorylated Akt, but not total Akt, in *FMRI* premutation ovaries (Fig. 6A). Given the known cross-talk between the Akt and mTOR pathways, we also examined the phosphorylation status of mTOR (35). Consistent with our findings with Akt, we found a dramatic reduction of phosphorylated mTOR protein in *FMRI* premutation ovaries (Fig. 6B). These observations together suggest that the Akt/mTOR-mediated signaling cascade is altered in *FMRI* premutation ovaries.

DISCUSSION

POI associated with *FMRI* premutation carriers, or FXPOI, is one of the most common known causes of 46,XX POI (14). While POI occurs in <1% of the normal female population, up to 24% of *FMRI* premutation carriers are affected. This phenotype is not observed in females with the full mutation and thus suggests that FXPOI is not due to reduced levels of FMRP (15). The molecular pathogenic mechanism(s) underlying FXPOI has(ve)s been elusive because of the lack of proper animal model. Here, we first documented that our mouse model carrying human *FMRI* premutation allele recapitulates FXPOI: female premutation mice show reduced fertility and altered gonadotropin hormone levels. Second, we found that *FMRI* premutation RNA alone is sufficient to impair female fertility, as FMRP levels were unaffected in our model. We show that *FMRI* premutation RNA has no impact on the establishment of the primordial follicle pools, but rather impairs the development of the growing follicles, and induces their apoptosis. We also reveal that phosphorylation of both Akt and mTOR proteins is significantly reduced in *FMRI* premutation ovaries. Our findings strongly

support a role of *FMRI* rCGG repeats in the pathogenesis of FXPOI, and suggest Akt/mTOR pathway as the potential therapeutic target for FXPOI.

The unique molecular signature associated with the *FMRI* premutation allele is that the level of *FMRI* mRNA is significantly elevated, while the production of FMRP is reduced. The latter is thought to be due to the long rCGG repeats impeding the translation initiation complex (8,21). Recent histological analyses revealed ovarian abnormalities in a mouse model with 130 CGG-CCG repeats in the endogenous *Fmr1* gene. However, whether both *FMRI* rCGG repeats and/or lower levels of Fmrp could contribute to FXPOI remains to be determined. In the transgenic mouse carrying a human YAC containing the premutation size of CGG repeats we used in this study, we saw significantly elevated mRNA levels of the *FMRI* gene. To detect the FMRP level, we used an antibody that recognized both human and mouse FMRP and found that the overall abundance of FMRP was unaltered in *FMRI* premutation mice. Since both WT copies of the murine *Fmr1* gene are present in *FMRI* X premutation mice, the molecular mechanism of this altered protein synthesis in the presence of human *FMRI* premutation gene needs further investigation. Nonetheless, this serendipitous observation gives us an excellent opportunity to determine the contribution *FMRI* mRNA with premutation rCGG repeats makes to FXPOI. Our results show that *FMRI* premutation RNA is sufficient to impair female fertility and cause POI. Previous work has shown that *FMRI* premutation rCGG repeats could sequester-specific RNA-binding proteins, such as Pur alpha and hnRNP A2/B1, and cause neurodegeneration associated with premutation carriers (22–27). It would be interesting and important to identify the protein(s) that could bind to *FMRI* rCGG repeats in ovaries and test whether the sequestration of these rCGG repeat-binding protein(s) could lead to FXPOI as well.

Our findings suggest that the *FMRI* premutation has no effect on the early primordial follicle pool, given that we found no apparent difference in the size and number of follicles between the premutation and the WT mice (2 days and

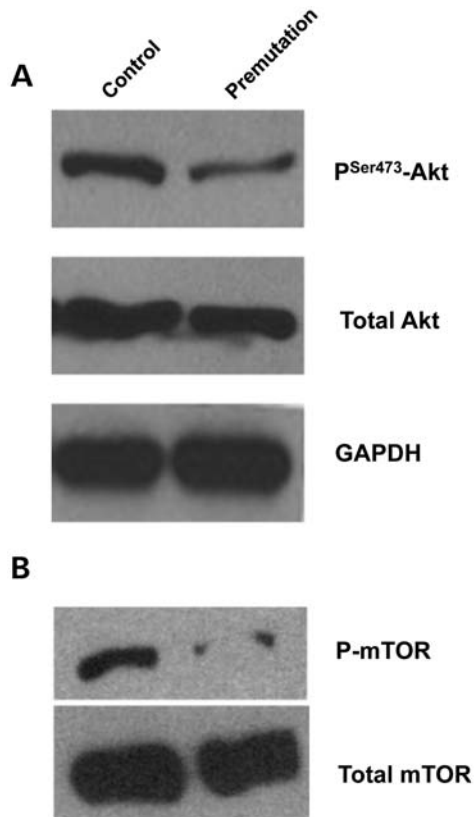


Figure 6. Reduced phosphorylation of Akt and mTOR in fragile X premutation ovaries. Ovaries were isolated from PD25 and adult (8–14 weeks) fragile X premutation mice and their WT littermates for western blot analyses. Levels of p-Akt (serine 473) and p-mTOR (serine 2448) as well as total Akt and mTOR are shown. GAPDH was used as a loading control. All experiments were repeated at least three times. Representative images are shown.

8 days), However, both the volume of ovaries and number of mature follicles in the premutation mice were markedly reduced compared with WT controls, raising the possibility that the premutation might block the development of mature follicles and/or increase the follicle apoptosis. The latter is supported by the results of our TUNEL assays that showed a strong signal of apoptosis in premutation ovaries. Moreover, we found that although the hormone 17β -E₂ levels were either increased or unchanged, FSH levels were significantly increased, indicative of the POF seen in clinics. Collectively, our data demonstrate the phenotype of POI in this mouse model.

Previous studies have shown that Akt functions as a key player to regulate growth and maturation of the ovary (33,34). Akt1 knockout (KO) females display reduced fertility and abnormal estrous cyclicity. Akt1 KO ovaries also have a reduced number of growing antral follicles, significantly larger primary and secondary oocytes and an increase in the number of degenerate oocytes. In addition, the mTOR pathway is required for a proper control of follicular granulosa cell proliferation and survival, and mTOR inhibition can result in a reduction in granulosa cell proliferation. Here, we show that the levels of phosphorylation of both Akt and mTOR in

FMRI premutation ovary were significantly reduced, which could explain the ovarian phenotypes we see in this FXPOI mouse model. It would be important to examine Akt and mTOR further in additional FXPOI mouse models, as well as human tissues, and determine whether the Akt/mTOR pathways could serve as a therapeutic target for FXPOI.

In summary, using a mouse model carrying human *FMRI* premutation allele, we show here that large rCGG tract in the premutation RNA alone is sufficient to impair female fertility. We show that *FMRI* premutation RNA has no impact on the establishment of the primordial follicle pools, but rather impairs the development of the growing follicles and induces their apoptosis. We further reveal that phosphorylation of both Akt and mTOR proteins is altered in *FMRI* premutation ovaries. Our findings strongly support a role for *FMRI* rCGG repeats in the pathogenesis of FXPOI and point to the Akt/mTOR pathway as a potential therapeutic target for FXPOI.

MATERIALS AND METHODS

Mice and sample collections

Transgenic mice carrying a YAC with the human premutation allele were described previously and used for this study (28). During the germline transmission, we saw no parent-of-origin effect or somatic instability. Large expansion events indicative of a transition from a premutation to a full mutation were not observed.

Vaginal smears were performed daily in the adult mice. Some transgenic mice do not exhibit an estrous phase, but display vaginal smears morphologically reminiscent of diestrus and proestrus, alternating between these phases, but without any regular cycle. Animals in groups of four or five were sacrificed at a stage of the proestrous cycle rather than at random for *FMRI* transgenic lines. Blood samples were obtained by enucleation of eyeball and allowed to clot; serum was stored at -80°C until assay. Body weight was measured and uterine weight recorded (uterine horns were not collected) as an index of estrogenicity.

Immunohistochemistry

Six-micrometer sections from paraffin-embedded ovaries were deparaffinized in xylene and rehydrated through a graded series of ethanol. Antigen retrieval was achieved by subjecting the sections to microwave irradiation for 15 min in 0.01 M citrate buffer (pH 6.0), 3% H₂O₂ for 10 min to eliminate endogenous hydrogen peroxidase activity. Sections were then sequentially incubated at room temperature with blocking 5% bovine serum albumin for 30 min, Fmrp antibody (Santa Cruz, 1 $\mu\text{g}/\text{ml}$) overnight at 4°C . After being washed with phosphate-buffered saline (PBS), the sections were incubated with biotinylated secondary antibody for 1 h and incubated with avidin–biotin–peroxidase complex for 1 h at room temperature. Final visualization of antigen was achieved by incubating sections with 3,3'-diamino-benzidine substrate solution for 5 or 8 min. The sections were then counterstained by hematoxylin and mounted for photography.

Morphologic classification of growing follicles and histological analyses

Ovaries were equilibrated in 30% sucrose overnight at 4°C and fixed for 6 h in 4% paraformaldehyde (pH 7.5), dehydrated and embedded in paraffin. Sections were taken at intervals of 28 µm, and every fifth section (7 µm), paraffin-embedded sections were mounted on slides. Routine hematoxylin and eosin staining was performed for histologic examination by light microscopy. Ovarian follicles at different developmental stages, including type 1, type 2, type 3a, type 3b, type 4, type 5a, type 5b, type 6, type 7, type 8 and CL, were based on the well-accepted standards established by Pedersen and Peters (29). Follicle numbers of the four serial biggest sections per ovary were evaluated, and at least five mice ovarian follicles were counted for each mouse genotype. Because of careful morphological analysis, the chances of counting the same follicle twice or missing a follicle were low.

Measurement of serum hormone levels

Adult *FMRI* transgenic mice and their WT littermate female mice were sacrificed at the proestrus stage (based on vaginal smears) in order to measure gonadotropin levels during the follicular growth phase, but not the ovulation phase. Some *FMRI* transgenic female mice were sacrificed randomly because of lack of regular estrus cycles. Serum was collected and stored at -80°C until assay. The levels of 17β-E₂, FSH and LH in the serum were measured with a commercial radioimmunoassay kit at a commercial laboratory (Chemclin Co., Beijing). The sensitivity of the E₂ assay is <3 pg/ml, that of the FSH assay <0.27 mIU/ml and that of the LH assay <0.3 mIU/ml. The intra-assay coefficient of variation (intra-assay CV) is <10%, and the inter-assay coefficient of variation (inter-assay CV) is under 15%.

TUNEL assay

A TUNEL assay was performed using an *in situ* apoptosis detection kit (Takara) according to the manufacturer's instructions. Briefly, paraffin-embedded ovaries were deparaffinized in xylene and rehydrated through a graded series of ethanol. Then, the sections were incubated in proteinase K (20 µg/ml, 15 min), followed by a TdT/reaction buffer mixture at 37°C for 2 h. The slides were then washed with PBS. The nuclei were stained with Hoechst 33342. The apoptotic cells with green fluorescence were examined by a Nikon Eclipse 80i fluorescence microscope (Tokyo, Japan).

RNA extraction and real-time PCR

Total RNA was isolated using *Trizol* (Invitrogen). One to two micrograms of total RNA from each sample were reverse-transcribed using oligo(dT)15 primer, transcriptase, reaction buffer and deoxynucleotide triphosphates to cDNA in a reaction volume of 20 µl. The real-time PCR were carried out using the Bio-Rad real-time PCR system, and the mRNA expression level was normalized against glyceraldehyde-3-phosphatedehydrogenase (GAPDH) mRNA level and analyzed using the comparative cycle threshold method.

Western blot analyses

Protein samples were separated on sodium dodecyl sulfate–polyacrylamide gel electrophoresis gels and then transferred to polyvinylidene difluoride membranes (Millipore). Membranes were processed following the enhanced chemiluminescence western blotting protocol (GE Healthcare). Anti-Akt, anti-phos-Akt, anti-mTOR and anti-phos-mTOR from cell signaling technology were used as primary antibodies at the dilutions recommended by the manufacturer. Horse-radish peroxidase-labeled secondary antibodies were obtained from Sigma (A0545) and used at a dilution of 1:5000. For loading controls, membranes were stripped and reprobed with the antibody against GAPDH (Ambion AM4300).

Gonadotropin-induced ovulation and size measurement of ovulated oocytes

To induce synchronized follicular growth and ovulation, immature 23-day-old female mice were injected i.p. with 5 IU of PMSG to stimulate follicular development, and with 5 IU hCG 48 h later to induce ovulation. Cumulus–oocyte complexes were recovered from oviducts 10–12 h after hCG treatment, and oocytes were freed of cumulus cells by a brief treatment with hyaluronidase (300 µg/ml) in M2 medium (Sigma). Seven mice of each genotype were super-ovulated, and five oocytes for each genotype were chosen randomly for measurement of diameters using a Zeiss AX10 microscope.

SUPPLEMENTARY MATERIAL

Supplementary Material is available at *HMG* online.

Conflict of Interest statement. None declared.

NOTE ADDED IN PROOF

Most recently Hoffman, Usdin and their colleagues showed ovarian abnormalities in another mouse model of FXPOI (36).

FUNDING

The authors thank D.L. Nelson for providing us with TG296 mice, K. Ye for sharing Akt/mTOR antibody with us and C. Strauss for critical reading of the manuscript. D.C. is supported by the Strategic Priority Research Program of the Chinese Academy of Sciences (XDA01010306), National Basic Research Program of China (2012CB944401) and Natural Science Foundation of China (91019022, 30825026 and 31130036). P.J. is supported by NIH grants (R01 NS051630 and R21 NS067461). D.C. and P.J. are supported by the National Natural Science Foundation of China 31028016.

REFERENCES

1. Nelson, L.M. (2009) Clinical practice. Primary ovarian insufficiency. *N. Engl. J. Med.*, **360**, 606–614.
2. Gallagher, J.C. (2007) Effect of early menopause on bone mineral density and fractures. *Menopause*, **14**, 567–571.

3. Jacobsen, B.K., Knutsen, S.F. and Fraser, G.E. (1999) Age at natural menopause and total mortality and mortality from ischemic heart disease: the Adventist Health Study. *J. Clin. Epidemiol.*, **52**, 303–307.
4. Mondul, A.M., Rodriguez, C., Jacobs, E.J. and Calle, E.E. (2005) Age at natural menopause and cause-specific mortality. *Am. J. Epidemiol.*, **162**, 1089–1097.
5. Papat, V.B., Calis, K.A., Vanderhoof, V.H., Cizza, G., Reynolds, J.C., Sebring, N., Troendle, J.F. and Nelson, L.M. (2009) Bone mineral density in estrogen-deficient young women. *J. Clin. Endocrinol. Metab.*, **94**, 2277–2283.
6. Lohff, J.C., Christian, P.J., Marion, S.L., Arrandale, A. and Hoyer, P.B. (2005) Characterization of cyclicity and hormonal profile with impending ovarian failure in a novel chemical-induced mouse model of perimenopause. *Comp. Med.*, **55**, 523–527.
7. Fu, Y.H., Kuhl, D.P., Pizzuti, A., Pieretti, M., Sutcliffe, J.S., Richards, S., Verkerk, A.J., Holden, J.J., Fenwick, R.G. Jr, Warren, S.T. *et al.* (1991) Variation of the CGG repeat at the fragile X site results in genetic instability: resolution of the Sherman paradox. *Cell*, **67**, 1047–1058.
8. Kenneson, A., Zhang, F., Hagedorn, C.H. and Warren, S.T. (2001) Reduced FMRP and increased FMR1 transcription is proportionally associated with CGG repeat number in intermediate-length and premutation carriers. *Hum. Mol. Genet.*, **10**, 1449–1454.
9. Kremer, E.J., Pritchard, M., Lynch, M., Yu, S., Holman, K., Baker, E., Warren, S.T., Schlessinger, D., Sutherland, G.R. and Richards, R.I. (1991) Mapping of DNA instability at the fragile X to a trinucleotide repeat sequence p(CCG)n. *Science*, **252**, 1711–1714.
10. Oberle, I., Rousseau, F., Heitz, D., Kretz, C., Devys, D., Hanauer, A., Boue, J., Bertheas, M.F. and Mandel, J.L. (1991) Instability of a 550-base pair DNA segment and abnormal methylation in fragile X syndrome. *Science*, **252**, 1097–1102.
11. Pieretti, M., Zhang, F.P., Fu, Y.H., Warren, S.T., Oostra, B.A., Caskey, C.T. and Nelson, D.L. (1991) Absence of expression of the FMR-1 gene in fragile X syndrome. *Cell*, **66**, 817–822.
12. Verkerk, A.J., Pieretti, M., Sutcliffe, J.S., Fu, Y.H., Kuhl, D.P., Pizzuti, A., Reiner, O., Richards, S., Victoria, M.F., Zhang, F.P. *et al.* (1991) Identification of a gene (FMR-1) containing a CGG repeat coincident with a breakpoint cluster region exhibiting length variation in fragile X syndrome. *Cell*, **65**, 905–914.
13. Sherman, S. (2002). In Hagerman, R.J. (ed.), *Fragile X Syndrome: Diagnosis, Treatment and Research*. The Johns Hopkins University Press, Baltimore, MD, pp. 136–168.
14. Sullivan, S.D., Welt, C. and Sherman, S. (2011) FMR1 and the continuum of primary ovarian insufficiency. *Sem. Reprod. Med.*, **29**, 299–307.
15. Sherman, S.L. (2000) Premature ovarian failure among fragile X premutation carriers: parent-of-origin effect? [comment] [editorial]. *Am. J. Hum. Genet.*, **67**, 11–13.
16. Allingham-Hawkins, D.J., Babul-Hirji, R., Chitayat, D., Holden, J.J., Yang, K.T., Lee, C., Hudson, R., Gorwill, H., Nolin, S.L., Glicksman, A. *et al.* (1999) Fragile X premutation is a significant risk factor for premature ovarian failure: the International Collaborative POF in Fragile X study—preliminary data. *Am. J. Med. Genet.*, **83**, 322–325.
17. Sullivan, A.K., Marcus, M., Epstein, M.P., Allen, E.G., Anido, A.E., Paquin, J.J., Yadav-Shah, M. and Sherman, S.L. (2005) Association of FMR1 repeat size with ovarian dysfunction. *Hum. Reprod.*, **20**, 402–412.
18. Murray, A., Ennis, S., MacSwiney, F., Webb, J. and Morton, N.E. (2000) Reproductive and menstrual history of females with fragile X expansions. *Eur. J. Hum. Genet.*, **8**, 247–252.
19. Hagerman, R.J. and Hagerman, P.J. (2002) The fragile X premutation: into the phenotypic fold. *Curr. Opin. Genet. Dev.*, **12**, 278–283.
20. Feng, Y., Zhang, F., Lokey, L.K., Chastain, J.L., Lakkis, L., Eberhart, D. and Warren, S.T. (1995) Translational suppression by trinucleotide repeat expansion at FMR1. *Science*, **268**, 731–734.
21. Tassone, F., Hagerman, R.J., Taylor, A.K., Gane, L.W., Godfrey, T.E. and Hagerman, P.J. (2000) Elevated levels of FMR1 mRNA in carrier males: a new mechanism of involvement in the fragile-X syndrome. *Am. J. Hum. Genet.*, **66**, 6–15.
22. Jin, P., Zarnescu, D.C., Zhang, F., Pearson, C.E., Lucchesi, J.C., Moses, K. and Warren, S.T. (2003) RNA-mediated neurodegeneration caused by the fragile X premutation rCGG repeats in *Drosophila*. *Neuron*, **39**, 739–747.
23. Willemsen, R., Hoogeveen-Westerveld, M., Reis, S., Holstege, J., Severijnen, L.A., Nieuwenhuizen, I.M., Schrier, M., van Unen, L., Tassone, F., Hoogeveen, A.T. *et al.* (2003) The FMR1 CGG repeat mouse displays ubiquitin-positive intranuclear neuronal inclusions; implications for the cerebellar tremor/ataxia syndrome. *Hum. Mol. Genet.*, **12**, 949–959.
24. Tassone, F., Iwahashi, C. and Hagerman, P.J. (2004) FMR1 RNA within the intranuclear inclusions of fragile X-associated tremor/ataxia syndrome (FXTAS). *RNA Biol.*, **1**, 103–105.
25. Arocena, D.G., Iwahashi, C.K., Won, N., Beilina, A., Ludwig, A.L., Tassone, F., Schwartz, P.H. and Hagerman, P.J. (2005) Induction of inclusion formation and disruption of lamin A/C structure by premutation CGG-repeat RNA in human cultured neural cells. *Hum. Mol. Genet.*, **14**, 3661–3671.
26. Jin, P., Duan, R., Qurashi, A., Qin, Y., Tian, D., Rosser, T.C., Liu, H., Feng, Y. and Warren, S.T. (2007) Pur alpha binds to rCGG repeats and modulates repeat-mediated neurodegeneration in a *Drosophila* model of fragile X tremor/ataxia syndrome. *Neuron*, **55**, 556–564.
27. Sofola, O.A., Jin, P., Qin, Y., Duan, R., Liu, H., de Haro, M., Nelson, D.L. and Botas, J. (2007) RNA-binding proteins hnRNP A2/B1 and CUGBP1 suppress fragile X CGG premutation repeat-induced neurodegeneration in a *Drosophila* model of FXTAS. *Neuron*, **55**, 565–571.
28. Peier, A.M. and Nelson, D.L. (2002) Instability of a premutation-sized CGG repeat in FMR1 YAC transgenic mice. *Genomics*, **80**, 423–432.
29. Pedersen, T. and Peters, H. (1968) Proposal for a classification of oocytes and follicles in the mouse ovary. *J. Reprod. Fertil.*, **17**, 555–557.
30. Gupta, S., Ramjaun, A.R., Haiko, P., Wang, Y., Warne, P.H., Nicke, B., Nye, E., Stamp, G., Alitalo, K. and Downward, J. (2007) Binding of ras to phosphoinositide 3-kinase p110alpha is required for ras-driven tumorigenesis in mice. *Cell*, **129**, 957–968.
31. Gonzalez-Robayna, I.J., Falender, A.E., Ochsner, S., Firestone, G.L. and Richards, J.S. (2000) Follicle-Stimulating hormone (FSH) stimulates phosphorylation and activation of protein kinase B (PKB/Akt) and serum and glucocorticoid-induced kinase (Sgk): evidence for a kinase-independent signaling by FSH in granulosa cells. *Mol. Endocrinol.*, **14**, 1283–1300.
32. Alam, H., Maizels, E.T., Park, Y., Ghaey, S., Feiger, Z.J., Chandel, N.S. and Hunzicker-Dunn, M. (2004) Follicle-stimulating hormone activation of hypoxia-inducible factor-1 by the phosphatidylinositol 3-kinase/AKT/Ras homolog enriched in brain (Rheb)/mammalian target of rapamycin (mTOR) pathway is necessary for induction of select protein markers of follicular differentiation. *J. Biol. Chem.*, **279**, 19431–19440.
33. Brown, C., LaRocca, J., Pietruska, J., Ota, M., Anderson, L., Smith, S.D., Weston, P., Rasoulpour, T. and Hixon, M.L. (2010) Subfertility caused by altered follicular development and oocyte growth in female mice lacking PKB alpha/Akt1. *Biol. Reprod.*, **82**, 246–256.
34. Fan, H.Y., Liu, Z., Cahill, N. and Richards, J.S. (2008) Targeted disruption of Pten in ovarian granulosa cells enhances ovulation and extends the life span of luteal cells. *Mol. Endocrinol.*, **22**, 2128–2140.
35. Yaba, A., Bianchi, V., Borini, A. and Johnson, J. (2008) A putative mitotic checkpoint dependent on mTOR function controls cell proliferation and survival in ovarian granulosa cells. *Reprod. Sci.*, **15**, 128–138.
36. Hoffman, G.E., Le, W.W., Entezam, A., Otuka, N., Tong, Z.B., Nelson, L., Flaws, J.A., McDonald, J.H., Jafar, S. and Usdin, K. (2012) Ovarian abnormalities in a mouse model of Fragile X primary ovarian insufficiency. *J. Histochem. Cytochem.*, **60**, 439–456.